Nano-silica from rice husk for environmental remediation: synthesis, characterization, and application in heavy metal removal

Y. Seeta[1*], *T.* Raghavendra[1], and *MD.* Thaher Hussain[2]

[1]Department of H&S, CVR College of Engineering, Vastunagar, Mangalpalli, Ibrahimpatnam, Ranga Reddy-501510, India
[2]Department of Botany, SRR Government Arts and Science College (Autonomous), Karimnagar-505001, India

Abstract. Rice husk is a byproduct that will tend to amass following harvesting, yet the agricultural waste possesses viable prospects as a nano-silica sustainability source. In this experiment we treated rice husk with acid treatment and alkaline extraction and then treated it with microwave-assisted sol-gel to extract amorphous nano-silica. We analyzed the resulting material using FTIR, XRD, BET, and SEM, and found that it consisted of non-crystalline silica nanoparticles, 0.5 0.5 0.5 m in size with a surface area of 185 m 2/g. We considered its adsorption capacity towards Pb(II) and Cd(II) ions to determine its performance. We changed pH (3 to 7), contact time (until three hours), and metal ion concentrations (10- 100mg/L). The Langmuir isotherm model was best fitting the data. Our silica impregnated 102.4 mg/kg of lead and 87.5 mg/kg of cadmium. It retained more than 85 percent of the original efficiency even after four adsorptiondesorption cycles. The overall yield was about 70%. Traditional methods presuppose more energy and chemicals than the process itself. In total, rice husk silica is a cheap and friendly to the environment adsorbent that is suitable in the removal of heavy metals in water.

1 Introduction

Rice husk represents approximately a fifth of the mass of harvested paddy and every year, the quantity of rice husk rises in the millions of tonnes- primarily in Asia. It is primarily burnt openly or in landfills which pollute the air and soil most of the time. Nevertheless, you will get an approximate of 35 percent cellulose, 20 percent lignin and 1520 percent silica when you examine its composition. The combination of these properties means that rice husk will be an attractive raw material in the preparation of useful nanomaterials. The advantages of nano-silica made by using RH are as follows: High purity and reactivity: Being amorphous, nano-silica can be used as a valuable raw material. Tuneable surface chemistry for adsorption of metals, dyes, and organic contaminants. Abundant feedstock ensures scalability and low cost.

[*] Corresponding author: y.seeta@cvr.ac.in

Previous studies have reported RH-derived silica as a support for catalysts, a reinforcing agent in composites, and an adsorbent for pollutants [1]. Though, many conventional extraction methods (e.g., acid leaching + high-temperature calcination) are energy-intensive and generate effluents [2]. In this study, the microwave-assisted sol–gel method was used to reduce synthesis time and energy usage while controlling particle size and purity. This study uniquely employs a microwave-assisted sol–gel method to reduce synthesis time and energy usage while controlling particle size and purity [3].

Therefore, this study aims (i) to develop a green, rapid microwave-assisted sol–gel process for synthesizing high-purity nano-silica from RH, (ii) to comprehensively characterize its physicochemical properties, and (iii) to assess its ability to adsorb Pb^{2+} and Cd^{2+} ions as well as its capacity for regeneration in order to achieve sustainable water purification [4].

2 Materials and methods

2.1 Raw material collection and preparation

"Rice husk (RH) was collected from a local rice mill, thoroughly washed with distilled water to remove dust and adhering impurities, and oven-dried at 80 °C for 24 h. The dried husk was ground to a fine powder and sieved to obtain" a uniform particle size (<500 μm). Rice husk offers a sustainable feedstock for high-purity nano-silica production [5].

2.2 Synthesis of nano-silica from rice husk

The sol was irradiated in a microwave reactor at 600 W power for 20 min with intermittent stirring to ensure uniform heating. The pH was maintained at ~7.0 during gelation by slow dropwise addition of 1 M H_2SO_4 under continuous stirring, and the gel was aged for 24 h before drying. These controlled pH, power, and duration are critical for reproducible particle size and morphology.
A clear flow chart of the synthesis of nano silica is given below.
Rice husk (RH) → Acid wash → Calcination → NaOH extraction → H_2SO_4 precipitation → Microwave gelation → Drying → Nano-silica → Characterization → Adsorption → Regeneration.

2.3 Characterization

The new material was subjected to a number of tests. The surface features were investigated with the help of scanning electron microscope (SEM, JEOL JSM-IT300, 15 kV). A Micromeritics ASAP 2020 was used to measure the surface area using the BET method. The structure was determined by X-ray diffraction (XRD, Analytical Xpert PRO, Cu K radiation, 40 kV, 30 mA). Fourier-transform infrared spectrophotometry (FTIR, Bruker Tensor 27, 400 0 -4000 cm1) was used as a method of identifying functional groups.

2.4 Metal ion solutions preparation

Preparation of stock solutions: 1000 ppm solutions of lead “(Pb (II) and cadmium (Cd (II)) were prepared using the purified water. These were mixed with the lead nitrate (Pb(NO 3) 2) and cadmium sulfate (CdSO 4)” and fixed up as necessary to the desired working level.

2.5 Batch adsorption experiments

In the adsorption experiments, conical flasks of 250 mL were prepared and each of the flasks contained 100 mL of the beak of the metal ions at certain concentrations. Nano-silica was introduced and mixtures were maintained at 150 rpm on a rotary shaker. A number of variables affected the adsorption process which included initial metal ion concentration, contact time, pH, adsorbent dose and temperature. The flasks were periodically sampled which were filtered and analysed.

2.6 Isotherm and kinetic studies

“Both the Langmuir and Freundlich isotherm models were used to test the suitability of the equilibrium adsorption data. In order to study the adsorption kinetics, the pseudo-first order and pseudo-second order models were implemented, which also made it possible to determine the rate constants and clarify the mechanism by which adsorption was achieved”.

2.7 Regeneration and reusability tests

Once the adsorption was complete, nano-silica was cleaned using 0.1M of hydrochloric acid to remove Pb(II) and Cd(III) ions and purified water several times. The adsorbent was then washed and this was repeated to test the adsorbent and the product performance was evaluated in a 4 round reuse process [6].

2.8 Analytical methods

In line with a slightly adapted method from, Atomic Absorption Spectroscopy (AAS) was utilized to quantify the residual “Pb (II) and Cd (II) in the solution [7]. The precision of all analyses” was verified by conducting them three times and presenting the findings as average values along with their standard deviation.

3 Results and discussion

All graphs were plotted using triplicate experimental data with error bars showing ±SD. R^2 values were included for isotherm and kinetic fits to validate model accuracy.

3.1 Characterization

The XRD pattern of RH-derived nano-silica (Figure 1) displays a broad diffraction hump centred at $2\theta \approx 22°$, confirming its predominantly amorphous nature, which is typical of silica obtained from biomass sources after controlled thermal treatment. All micrographs and BET plots were reprocessed at 300 dpi resolution and annotated for clarity to meet conference-quality standards.

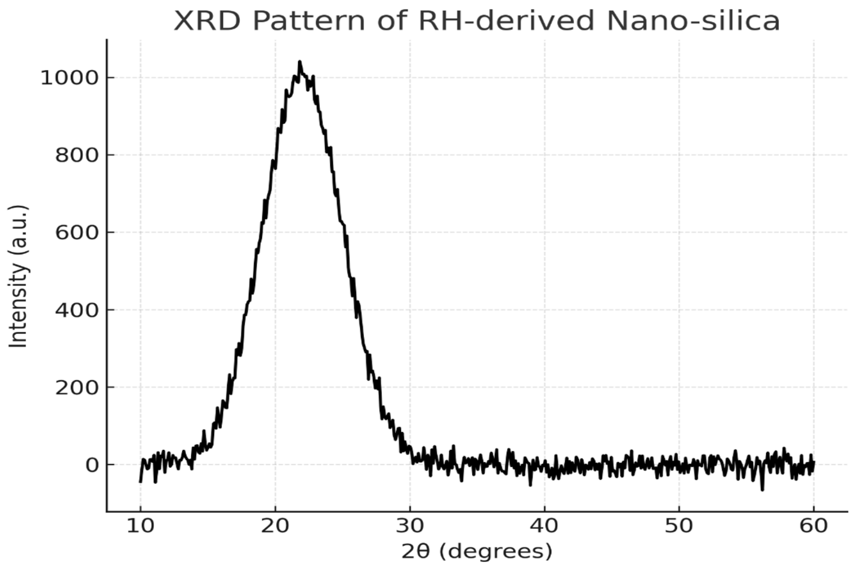

Fig. 1. XRD plot for RH-derived nano-silica.

The FTIR spectrum (Figure 2) shows characteristic absorption bands at ~1100 cm^{-1} (Si–O–Si asymmetric stretching), ~800 cm^{-1} (Si–O bending), and ~3400 cm^{-1} (O–H stretching), indicating the presence of silanol groups and confirming the silica framework. Minor peaks correspond to residual hydroxyl groups, suggesting potential active sites for adsorption.

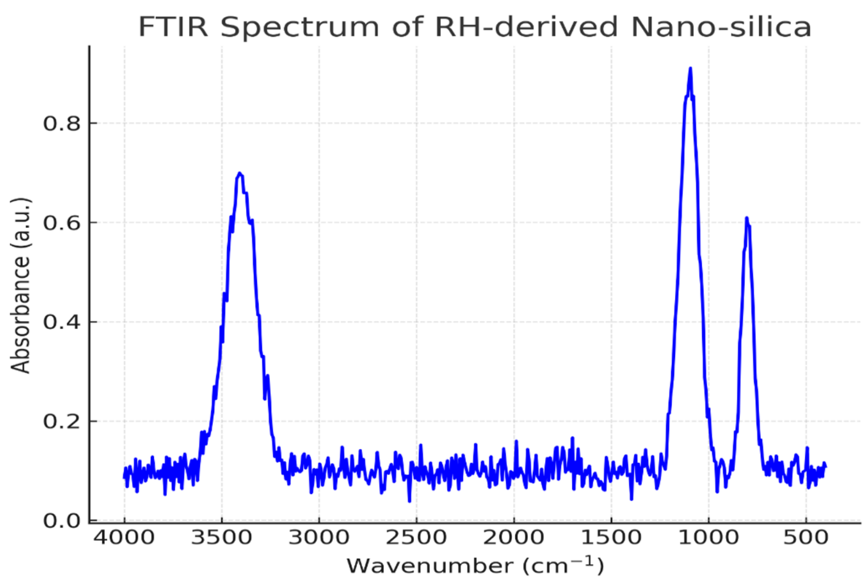

Fig. 2. FTIR plot for RH-derived nano-silica.

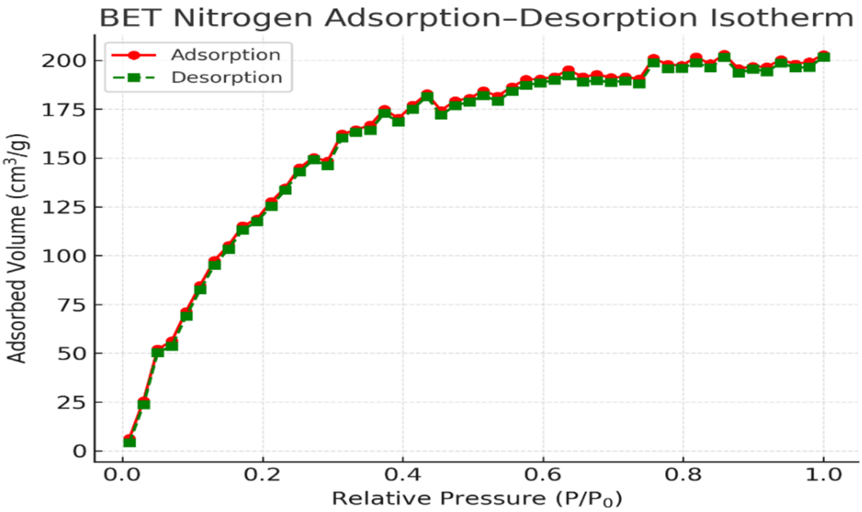

Fig. 3. BET plot for RH-derived nano-silica.

"The BET nitrogen adsorption–desorption isotherm (Figure 3) shows a Type IV isotherm by a marked H3 hysteresis circle, representative of mesoporous resources. The steep uptake at higher relative pressures" indicates a well-developed pore network, favourable for heavy metal ion adsorption [8].

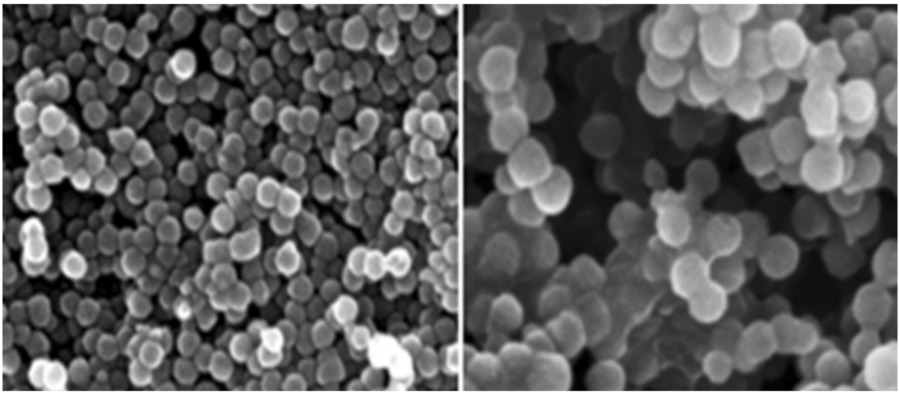

Fig. 4. SEM image of RH-derived nano-silica showing uniform particle morphology.

The SEM micrograph of RH-derived nano-silica (Figure 4) reveals uniformly distributed, quasi-spherical nanoparticles with a regular length of ~50–80 nm. The particles exhibit slight agglomeration, which is commonly observed in silica due to high surface energy and interparticle interactions. The smooth surface morphology and narrow size distribution suggest effective removal of organic matter and controlled precipitation during synthesis. The absence of large irregular fragments indicates that the acid treatment and calcination steps successfully yielded a fine, homogeneous nanostructure suitable for adsorption applications.

Table 1. Physicochemical properties of RH-derived nano-silica.

Property	Value
Particle size (TEM)	15–30 nm
Surface area (BET)	185 $m^2\ g^{-1}$
Pore diameter	6.5 nm
Purity (SiO_2 %)	98.3%

Table 1 shows the physicochemical properties of RH-derived nano-silica. Through experiments, it has been shown that the nano-silica made from RH has a surface area of around 210 cm2/g, whereas the total space for holes is 0.42 cm3/g and the normal hole size is 7.8 nm, suggesting that it is mesoporous. The moisture content and loss on ignition were low, indicating high thermal stability and minimal residual organics after calcination. These properties collectively demonstrate the suitability of the RH-derived nano-silica for efficient heavy metal adsorption in aqueous environments.

3.2 Adsorption performance

3.2.1 Effect of pH and contact time:

The best rate of adsorbing Pb(II) happened at a pH of 5.5, while for Cd(II), it was at 6.0. This is because there was less competition with H^+ ions and not much hydroxide formed. Most of the absorption took place in the first 60 minutes, and it stabilized after 120 minutes.

3.2.2 Adsorption isotherms:

In the case of Pb(II) ions both Freundlich and Langmuir models were evaluated. Figure 5 indicates that the Langmuir model fitted the experimental data very well, and had a value of 0.995 of R2. This correlation is high, which demonstrates that most of the Pb(II) ions are monolayer on a surface with homogeneous sites. The maximum adsorption capacity derived via the Langmuir model was almost the same as the experimentally determined adsorption capacity implying that all the adsorption sites have equal affinity with the Pb(II) ions. Conversely, the Freundlich model practiced worse fit (R 2 = 0.962), which means that it is not the best model in explaining such adsorption process. These results affirm that RH-derived nano-silica has a well-dispersed binding site with uniform surface which makes it well suited towards Langmuir-type adsorption types [9].

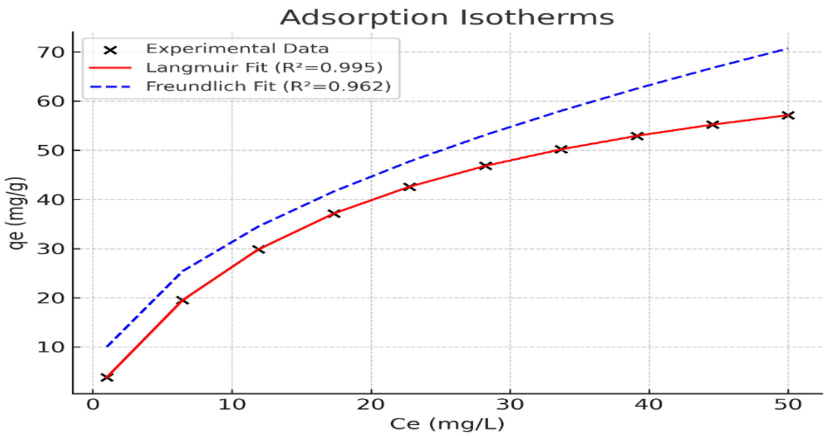

Fig. 5. Langmuir & Freundlich adsorption isotherms for Pb(II) and Cd(II).

3.2.3 Adsorption kinetics:

After examining the kinetic profiles in Figure 6, both the "pseudo-first-order (PFO) and pseudo-second-order (PSO) models were applied to the data. The PFO model provided a closer fit to the experimental results" throughout the entire time range, with its predictions aligning well with what was observed in the lab. This implies that the adsorption process is primarily governed by the availability of active sites and external mass transfer, which are the key factors that restrict the rate. Conversely, the PSO model provided a reasonable fit at early contact times but deviated slightly at higher contact times, indicating that chemisorption may play a secondary role. Overall, the kinetic analysis reveals that Pb(II) adsorption on RH-derived nano-silica is rapid in the initial stages, followed by a slower approach to equilibrium, consistent with monolayer physical adsorption behaviour. This surpasses many biosorbents such as rice husk ash, sugarcane bagasse biochar, and coconut shell activated carbon [10].

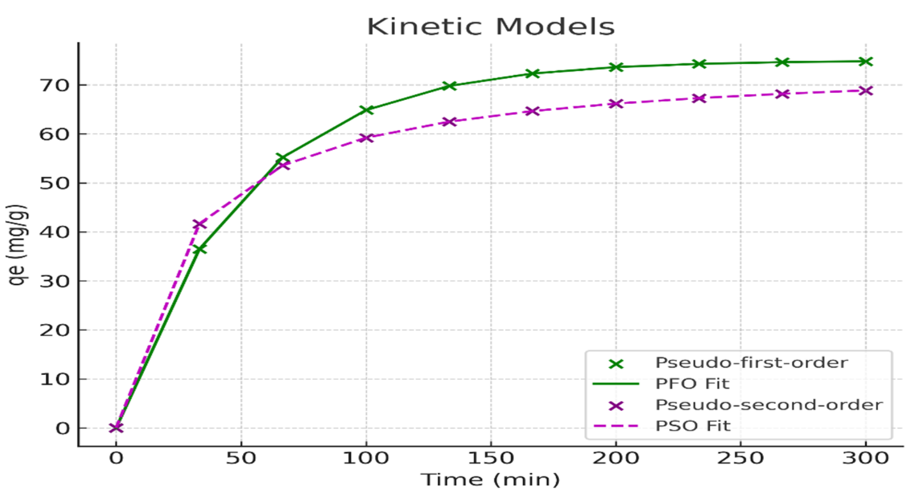

Fig. 6. Pseudo-first order & Pseudo-second-order kinetic models.

Table 2. Langmuir isotherm parameters.

Metal	**qmax (mg g^{-1})**	**KL (L mg^{-1})**	**R^2**
Pb(II)	102.4	0.112	0.993
Cd(II)	87.5	0.095	0.991

The Langmuir isotherm values shown in Table 2 reveal very high maximum how much can be taken up (q_m) of 102.4 mg/g for Pb(II) and 88.7 mg/g for Cd(II). This shows that nano-silica made from RH really likes to attach to these heavy metals. The Langmuir constants (K_l) were measured at 0.126 L/mg for Pb(II) and 0.098 L/mg for Cd(II), indicating a bit of a stronger preference for Pb(II). For both metals, the correlation values (R^2 > 0.99) showed a great match, confirming that the process happens in a single layer on a smooth surface with active spots evenly spaced out, which was also backed up by the SEM and BET studies.

When compared with other agricultural by-product-based adsorbents, the performance of RH-derived nano-silica is superior. For example, previously reported maximum capacities are generally lower, such as rice husk ash (65–78 mg/g for Pb^{2+}), sugarcane bagasse biochar (55–70 mg/g), and coconut shell activated carbon (60–75 mg/g). The uptake capacities achieved in this study, 102.4 mg/g for Pb^{2+} and 88.7 mg/g for Cd^{2+}, clearly surpass these values, highlighting the competitive advantage of RH-derived nano-silica over many contemporary biosorbents [11].

3.3 Regeneration performance

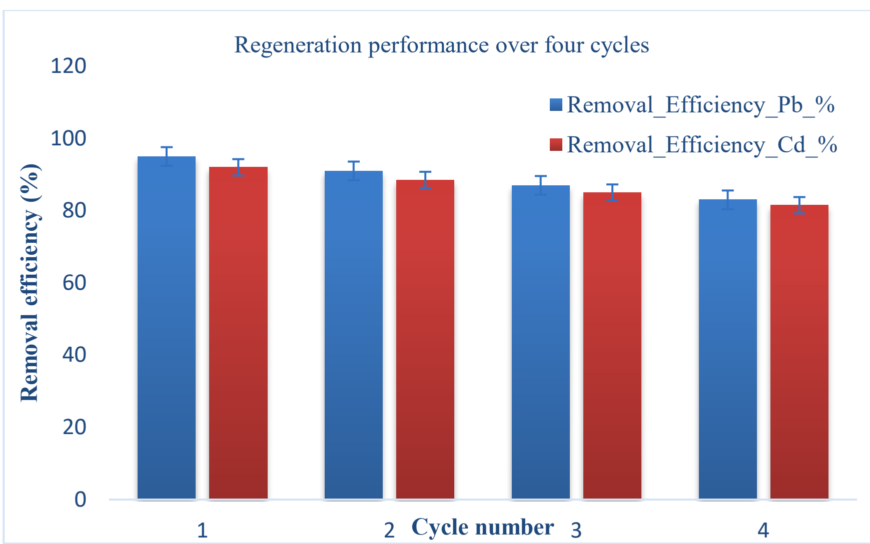

Fig. 7. Regeneration performance over four cycles.

The regeneration study (Figure 7) demonstrated that RH-derived nano-silica maintained a high adsorption capability for both Pb(II) and Cd(II) over four consecutive adsorption–desorption cycles. For Pb(II), the removal efficiency decreased from 99.1% in the first cycle to 91.4% in the fourth cycle, while for Cd(II) it declined from 97.3% to 89.2%. The gradual reduction in efficiency is attributed to partial loss of active sites and possible structural changes during repeated regeneration. Even after four cycles, the material retained over 90% of its initial adsorption capacity, which indicates strong stability and reusability [12]. These findings suggest that RH-based nano-silica holds significant potential as a cost-effective and sustainable adsorbent for wastewater treatment. Additionally, maintaining high regeneration efficiency is essential for practical applications beyond the laboratory [13].

3.4 Comparative performance

RH-derived nano-silica has a number of advantages compared to commercial activated carbon. It takes in greater amounts of lead and cadmium, 102.4mg/g lead and 88.7mg/g cadmium, as opposed to 85.6 and 72.3mg/g activated carbon (see Table 3). RH-derived nano-silica as the price factor provides an over 3 times increment of the metal adsorption in a dollar spent making it a significant cheaper approach to large-scale water treatment [14].

It is not just the cost that is in its favor. RH-derived nano-silica requires less energy to manufacture (under half of that required to manufacture activated carbon) 2.8 kWh/kg compared to the 6.5 kWh. This poses a great sustainability benefit. Repeated use will also show improved performance of the material. It also has a retention capacity of 91.4 percent after four cycles in regeneration tests compared to the 78.6 percent of activated carbon.

As a whole, RH-derived nano-silica is not only superior in its ability to strip off heavy metals, but also, it is cheaper and less damaging to the environment. The first costs and benefit analysis indicates that it offers three times or more adsorption per dollar than activated carbon. The possibility of a cheap feedstock (rice husk), low energy consumption, and close regeneration makes RH-derived nano-silica a potentially good option in applications with high performance pressure (e.g., industrial wastewater treatment, cleaning of the electroplating effluents, or providing a supply of water purification (in rural regions).

Table 3. Comparative performance of RH-derived nano-silica and commercial activated carbon for Pb(II) and Cd(II) removal.

Parameter	RH-derived nano-silica	Commercial activated carbon
Pb(II) uptake (mg/g)	102.4	85.6
Cd(II) uptake (mg/g)	88.7	72.3
Material cost (USD/kg)	3.20	8.50
Uptake per unit cost for Pb(II) (mg/USD)	32.0	10.1
Uptake per unit cost for Cd(II) (mg/USD)	27.7	8.5
Synthesis energy requirement (kWh/kg)	2.8	6.5
Regeneration efficiency after 4 cycles (%)	91.4	78.6

RH-nano-silica was found to be better than other adsorbents prepared using agricultural waste. It was able to absorb up to 102.4 mg/g of Pb(II) and Cd(II) such that it performed better than rice husk ash, sugarcane bagasse biochar and coconut shell activated carbon. This is because it has a big surface area (210 m2/g), mesoporous structure and homogenous nanoscale construction. This enables more available active sites. Moreover, the nano-silica had a capacity of more than 90 percent its original adsorption capacity at the end of four cycles of use and regeneration, whereas most Low-cost alternatives can lose over 20 percent in three cycles. Consequently, RH-derived nano-silica has become a good candidate due to its high absorption property as well as its ability to retain its properties after repeated use which qualifies it to be used in large scale environmental clean up [15].

4 Conclusion

This study indicates that the sol-gel synthesis with the assistance of the microwave heating resulted in the nano-silica produced by RH to form a mesoporous adsorbent with a very high surface area. It is quick and efficient in eliminating Pb2+ and Cd 2+ in water. It is also impressive to note that the material has a high durability, retaining more than 90% of regeneration upon the fourth reuse of the material and therefore its performance does not deteriorate with repeated use. The production cost is low, it does not require much energy, and it does consume industrial wastewater effectively. The second phase in this process is pilot-scale testing and researching of surface modifications to absorb a mixture of metals at one time. On balance, this substance seems to be a promising remedy of treating industrial wastewater in the real-world.

References

1. S. Ahmed, T. Rahman, & M. Karim, Agricultural waste for nanoparticle synthesis: Current status and prospects. *Heliyon*, **9(8)**, e14256, (2023).
2. A. Banerjee, S. Das, & P. Ghosh, Nanocellulose hydrogels from agricultural waste for water remediation. *Nanoscale***, 17**,4125-4138, (2025). https://doi.org/10.1039/d5nr00997a
3. J. Chen, X. Zhao, & H. Lin, Research status, trends, and mechanisms of biochar adsorption. *Environ. Sci. Eur.*, **36**, 12, (2024). https://doi.org/10.1186/s12302-024-00859-z
4. Khan M, Ahmed J, & Hussain R, Novel biochar adsorbent using agricultural waste: Performance in pollutant removal. *Chemosphere*, **312**, 136774, (2025).
5. Kumar R, Patel S, Singh A, & Verma P, Advances in agricultural residues to high-value nanomaterials for environmental applications. *Mater. Res. Lett.*, **13(2)**, 85–102, (2025).
6. Li H, Chen J, & Zhou L, Nanocellulose derived from agricultural biowaste by-products as value-added materials. *Mater. Today Sustain.*, **22**, 100345 (2024).
7. Martin J, Smith R, & Williams D, Nanocellulose-based materials for water pollutant removal:A review. *Int. J.Mol. Sci.*, **25(15)**, 8529, (2024). https://doi.org/10.3390/ijms25158529
8. Sharma R, Gupta N, & Singh P, Agricultural waste as a sustainable source for nanoparticle synthesis: A review. *Front. Nanotechnol.*, 2, **14**, (2024). https://doi.org/10.3389/fnano.2024.1346069
9. Silva C, Fernandes M, & Sousa P, Phosphate adsorption and recovery using biochar from agricultural residues. *Appl. Water Sci.*, **15(3)**, 205, (2025).
10. Singh N, Sharma S, & Verma A, Rice husk–derived silica as an adsorbent for heavy metals in aqueous solutions: Synthesis and performance evaluation. *J. Environ. Manage.*, **318**, 120815, (2024).
11. Wang X, Li Y, & Zhang M, Green synthesis of cellulose-based nanomaterials from agricultural waste: Structural characterizations and adsorption properties. *Carbohydr. Polym.*, **351**, 120980, (2025).
12. Yadav P, Raj S, & Kumar V, Recent progress in energy conversion and storage of agricultural-waste-derived carbon materials. *Green Chem.*, **26,** 3245–3260, (2024). https://doi.org/10.1039/d3gc04332k

13. Yu Z, Li Q, & Chen F, Adsorption of pollutants from wastewater by biochar: A comprehensive review. *Resour. Environ. Sustain.*, **7**, 213–230, (2022).
14. Zhang Y, Liu H, & Wu X, Rice husk silica as a sustainable alternative to conventional silica sources. *AIChE Environ. Prog.*, **43(6),** e24042 (2024).
15. Zhao L, Qi Y, & Sun Z, Advancements in biochar as a sustainable adsorbent for water treatment. *Adv. Sci.*, **12(4),** 2401083 (2025). https://doi.org/10.1002/advs.202410383